



**HAL**  
open science

## Characterization of the Amino Acids from *Neisseria meningitidis* Methionine Sulfoxide Reductase B Involved in the Chemical Catalysis and Substrate Specificity of the Reductase Step

Fabrice Neiers, Sanjiv Sonkaria, Alexandre Olry, Sandrine Boschi-Muller, Guy Branlant

### ► To cite this version:

Fabrice Neiers, Sanjiv Sonkaria, Alexandre Olry, Sandrine Boschi-Muller, Guy Branlant. Characterization of the Amino Acids from *Neisseria meningitidis* Methionine Sulfoxide Reductase B Involved in the Chemical Catalysis and Substrate Specificity of the Reductase Step. *Journal of Biological Chemistry*, 2007, 282 (44), pp.32397-32405. 10.1074/jbc.M704730200 . hal-01690652

HAL Id: hal-01690652

<https://hal.univ-lorraine.fr/hal-01690652>

Submitted on 23 Jan 2018

**HAL** is a multi-disciplinary open access archive for the deposit and dissemination of scientific research documents, whether they are published or not. The documents may come from teaching and research institutions in France or abroad, or from public or private research centers.

L'archive ouverte pluridisciplinaire **HAL**, est destinée au dépôt et à la diffusion de documents scientifiques de niveau recherche, publiés ou non, émanant des établissements d'enseignement et de recherche français ou étrangers, des laboratoires publics ou privés.



Distributed under a Creative Commons Attribution 4.0 International License

# Characterization of the Amino Acids from *Neisseria meningitidis* Methionine Sulfoxide Reductase B Involved in the Chemical Catalysis and Substrate Specificity of the Reductase Step\*

Received for publication, June 8, 2007, and in revised form, August 23, 2007. Published, JBC Papers in Press, August 31, 2007, DOI 10.1074/jbc.M704730200

Fabrice Neiers<sup>1</sup>, Sanjiv Sonkaria<sup>2</sup>, Alexandre Olry, Sandrine Boschi-Muller, and Guy Branlant<sup>3</sup>

From the Maturation des ARN et Enzymologie Moléculaire, Unité Mixte de Recherche CNRS-UHP 7567, Nancy Université, Faculté des Sciences et Techniques, Boulevard des Aiguillettes, BP 239, 54506 Vandoeuvre-les-Nancy, France

Methionine sulfoxide reductases (Msrs) are antioxidant repair enzymes that catalyze the thioredoxin-dependent reduction of methionine sulfoxide back to methionine. The Msr family is composed of two structurally unrelated classes of enzymes named MsrA and MsrB, which display opposite stereoselectivities toward the *S* and *R* isomers of the sulfoxide function, respectively. Both classes of Msr share a similar three-step chemical mechanism involving first a reductase step that leads to the formation of a sulfenic acid intermediate. In this study, the invariant amino acids of *Neisseria meningitidis* MsrB involved in the reductase step catalysis and in substrate binding have been characterized by the structure-function relationship approach. Altogether the results show the following: 1) formation of the MsrB-substrate complex leads to an activation of the catalytic Cys-117 characterized by a decreased  $pK_{app}$  of  $\sim 2.7$  pH units; 2) the catalytic active MsrB form is the Cys-117<sup>-</sup>/His-103<sup>+</sup> species with a  $pK_{app}$  of 6.6 and 8.3, respectively; 3) His-103 and to a lesser extent His-100, Asn-119, and Thr-26 (via a water molecule) participate in the stabilization of the polarized form of the sulfoxide function and of the transition state; and 4) Trp-65 is essential for the catalytic efficiency of the reductase step by optimizing the position of the substrate in the active site. A scenario for the reductase step is proposed and discussed in comparison with that of MsrA.

Methionine residues in proteins are susceptible to oxidation to methionine sulfoxide (MetSO)<sup>4</sup> by reactive oxygen species. This post-translational oxidative damage has been implicated

in a variety of age-related diseases (1–4). In this context, the repair of oxidized protein-bound MetSO back to methionine by methionine sulfoxide reductases (Msr) can be considered as a means of antioxidant defense (5–10). It has also been described to be a component of the mechanisms used by pathogenic bacteria of the genus *Neisseria* to infect host cells, and thus to be a key factor in the virulence of these bacteria (11).

There exists two structurally unrelated classes of Msrs called MsrA and MsrB (12–15), which reduce free and protein-bound Met-(*S*)-SO and Met-(*R*)-SO, respectively, and display a similar three-step mechanism (16–19). The first step, *i.e.* the reductase step that is not rate-limiting, leads in both cases to the formation of a sulfenic acid intermediate and release of 1 mol of Met per mol of Msr. Recently, the role of invariant amino acids of the MsrA domain of the PilB protein of *Neisseria meningitidis* involved in the chemical catalysis of the reductase step was investigated by comparing the kinetic properties of the wild type to those of several mutated Msrs (20, 21). A scenario of the reductase step was thus proposed in which the substrate binds to the active site with its sulfoxide function largely polarized via interactions with invariant amino acids, the role of which is to stabilize the transition state of the sulfurane type. In this scenario, the stabilization of the thiolate form of the catalytic Cys is proposed to be substrate-assisted by the positive charge borne by the sulfur of a sulfoxide. This scenario implies a transfer of the hydrogen of the catalytic Cys to the oxygen of the sulfoxide function via an acid-base catalyst, which is likely to be a Glu residue. In parallel with this study, recent work was also done to characterize the amino acids involved in MetSO recognition (22). In particular, the hydrophobic pocket composed of the side chains of a Trp and a Phe residue was shown to be essential in positioning the substrate for efficient catalysis of the reductase step via van der Waals interactions with the  $\epsilon$ -methyl group of the substrate.

In contrast, no information is available on the nature of the amino acids and how they operate in catalysis of the reductase step and on the structural factors involved in recognition of the substrate in MsrB. Only the three-dimensional structure of the MsrB domain of the PilB protein of *Neisseria gonorrhoeae*, which differs from that of the *N. meningitidis* MsrB domain by only two amino acids, has been determined by x-ray so far (23). One of the MsrB domains in the asymmetric unit has a cacodylate molecule bound. This cacodylate mole-

\* This work was supported in part by the CNRS, the University of Nancy I, the Institut Fédératif de Recherche 111 Bioingénierie, the Association pour la Recherche sur le Cancer Grant ARC 5436, and the French Ministry of Research Grants ACI BCMS047 and ACI IMPBio SIRE. The costs of publication of this article were defrayed in part by the payment of page charges. This article must therefore be hereby marked "advertisement" in accordance with 18 U.S.C. Section 1734 solely to indicate this fact.

<sup>1</sup> Supported by the French Ministry of Research.

<sup>2</sup> Supported by the University of Nancy I and the Region Lorraine.

<sup>3</sup> To whom correspondence should be addressed: Maturation des ARN et Enzymologie Moléculaire, UMR CNRS-UHP 7567, Nancy Universités, Faculté des Sciences et Techniques, Blvd. des Aiguillettes, BP 239, 54506 Vandoeuvre-les-Nancy, France. Tel.: 33-3-83-68-43-04; Fax: 33-3-83-68-43-07; E-mail: Guy.Branlant@maem.uhp-nancy.fr.

<sup>4</sup> The abbreviations used are: MetSO, methionine sulfoxide; Msr, methionine sulfoxide reductase; Trx, thioredoxin; 2-PDS, 2,2'-dipyridyl disulfide; AcMetSONHMe, Ac-L-Met-(*RS*)-SO-NHMe; AcMetNHMe, Ac-L-Met-NHMe.

## Catalytic Mechanism of MsrB Reductase Step

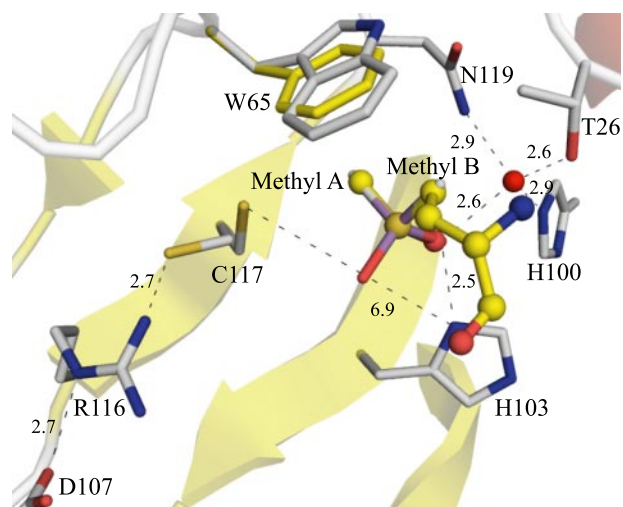


**FIGURE 1. Schematic representation of the active site of *N. gonorrhoeae* MsrB containing a cacodylate molecule and in which a MetSO substrate is modeled (Protein Data Bank code 1L1D (23)).** The residues Thr-26, Trp-65, His-100, His-103, Asp-107, Arg-116, and Cys-117 and the cacodylate molecule are shown in stick representation with gray carbon. The side chain of Cys-117 adopts two alternative conformations. The two methyl groups of the cacodylate molecule mimic the  $\epsilon$ -methyl (methyl A) and the  $\gamma$ -methylene group (methyl B) of the L-Met-(R)-SO substrate. The L-Met-(R)-SO was superimposed on to the cacodylate molecule present in the MsrB crystal structure (23) using Turbo-Frodo, whereas the L-Met-(S)-SO cannot be modeled in the active site. L-Met-(R)-SO is shown in ball and stick representation with yellow carbon. The substitution of Trp-65 by a Phe residue was modeled with the PyMol program (Delano Scientific LLC) and is shown in a yellow stick representation. The water molecule present in the active site of MsrB in the crystal structure is also represented by a red sphere and hydrogen bonds are shown as black dashed lines with distances indicated in Å. The figure was generated using the PyMol program (Delano Scientific LLC).

cule is a good mimic of a MetSO-bound active site, which is surface-exposed. As shown in Fig. 1, methyls (designated A and B) represent the  $\epsilon$ -methyl and the  $\gamma$ -methylene of MetSO, respectively, whereas the A atom and one of the oxygen atoms mimic the sulfur and the oxygen of the sulfoxide function, respectively. The methyl groups of cacodylate are located in a cavity described to be formed by the side chains of Cys-117<sup>5</sup> and Trp-65, whereas the oxygen atom that mimics the oxygen of the sulfoxide interacts through a hydrogen-bonding network with His-103 and with Thr-26, His-100, and Asn-119 but in this case via a water molecule. Finally, inspection of the x-ray structure shows a Cys-117, Arg-116, Asp-107 triad that was postulated to activate the catalytic Cys-117 (23).

In this study, in view of the structural information, all these residues of the MsrB domain of the *N. meningitidis* PilB were substituted. The kinetic parameters were determined for all mutated MsrBs and compared with those of the wild type. The pH dependence of the rate constant of the reductase step of H103N and R116L MsrBs was also determined and compared with that of the wild type. Two major results of this study are as follows: 1) the catalytic active form of MsrB in the reductase step is the Cys-117<sup>-</sup>/His-103<sup>+</sup> with pK<sub>app</sub> values of 6.7 and 8.3, respectively; 2) activation of Cys-117 does not involve Arg-116 and Asp-107 as postulated previously but is rather substrate-assisted via the polarized form of the sulfoxide function of the

substrate. Taking into account all the results, a scenario for the catalysis is proposed in comparison with that of MsrA and is discussed in terms of evolution not only for catalysis but also for substrate recognition.

## EXPERIMENTAL PROCEDURES

**Site-directed Mutagenesis, Production, and Purification of Enzymes**—The *Escherichia coli* BE002 strain (MG1655 *msrA::specΩ*, *msrB::α3kan*) was used for all *N. meningitidis* MsrB productions, transformed with the plasmidic construction pSKPILBMsrb containing only the coding sequence of *msrB* under the *lac* promoter (17). The BE002 strain was kindly provided by Dr. F. Barras. Its use prevented expression of endogenous wild-type MsrA and MsrB from *E. coli*, and thus all preparations were devoid of contaminating activity by the Msrs from *E. coli*. Site-directed mutageneses were performed using the QuikChange site-directed mutagenesis kit (Stratagene).

Purification of the wild-type MsrB was performed as described previously (17). In the case of mutated MsrBs, the enzymes were produced as a nonsoluble form. Pellets obtained after sonication and centrifugation were resuspended in a minimal volume of buffer A (50 mM Tris-HCl, 2 mM EDTA, pH 8) containing 20 mM dithiothreitol and 6 M urea, and then dialyzed twice against buffer A containing 3 and 0 M urea, successively. The solution was then applied successively onto an ACA 54 resin, a Q-Sepharose column, and a phenyl-Sepharose column (Amersham Biosciences) as described previously for the wild type (17).

Purity of wild-type and mutated MsrBs was checked by electrophoresis on a 15% SDS-PAGE followed by Coomassie Brilliant Blue R-250 staining and by electrospray mass spectrometry analyses. Storage of the enzymes was done as described previously (17). The molecular concentration was determined spectrophotometrically, using extinction coefficient of 17,330 M<sup>-1</sup>·cm<sup>-1</sup> at 280 nm for wild-type and mutated MsrBs except for W65A and W65F MsrBs for which an extinction coefficient of 11,580 M<sup>-1</sup>·cm<sup>-1</sup> was used. Trx1 and Trx reductase from *E. coli* were prepared following experimental procedures described previously (24, 25).

**pH Dependence of MsrB Thiol Reaction Rates with 2,2'-Dipyridyl Disulfide (2-PDS)**—Kinetic measurements of MsrB reaction with 2-PDS were carried out on an SX18MV-R stopped-flow apparatus (Applied PhotoPhysics). Kinetic reactions were performed at 25 °C, under pseudo-first-order conditions at a constant ionic strength of 0.15 M over the pH range 7.25–9.5 with polybuffer B (120 mM Tris, 30 mM imidazole, 30 mM acetic acid). One syringe was filled with wild-type or Cys to Ser mutated MsrBs, and the other was filled with 2-PDS. MsrB and 2-PDS concentrations after mixing were 10 and 310 μM, respectively. Release of pyridine-2-thione was followed at 343 nm using an extinction coefficient of 8080 M<sup>-1</sup>·cm<sup>-1</sup>.

The pseudo-first-order rate constant  $k_{\text{obs}}$  was determined at each pH by fitting the absorbance ( $A$ ) at 343 nm versus time ( $t$ ) to monoexponential Equation 1, where  $a$  is the burst amplitude and  $c$  is the end point.

$$A = a(1 - e^{-k_{\text{obs}}t}) + c \quad (\text{Eq. 1})$$

The second-order rate constant  $k_2$  was calculated by dividing the  $k_{\text{obs}}$  value by the concentration of 2-PDS.  $k_2$  versus pH

<sup>5</sup> In this paper, *N. meningitidis* MsrB amino acid numbering is based on the *E. coli* MsrB sequence devoid of the N-terminal Met.

profiles fitted to Equation 2 for one- $pK_a$  profiles, in which  $k_{2(\max)}$  represents the second rate constant for the thiolate form.

$$k_2 = \frac{k_{2(\max)}}{1 + 10^{(pK_a - \text{pH})}} \quad (\text{Eq. 2})$$

**Kinetics in the Presence of the Trx Recycling System**—Kinetics in the presence of the Trx recycling system were carried out with 400 mM Ac-L-Met-(RS)-SO-NHMe (AcMetSONHMe) as a substrate and 100  $\mu\text{M}$  *E. coli* Trx1 as a reductant in the presence of the Trx recycling system (1.28  $\mu\text{M}$  *E. coli* Trx reductase and 0.3 mM NADPH), as described previously (17). AcMetSONHMe was prepared from Ac-L-Met-OMe (Bachem) as described previously (26). Purity of AcMetSONHMe was assessed by proton NMR analysis.

**Kinetics of the First Step in the Absence of Reductant by Single Turnover Fluorescence Experiments at pH 8**—Kinetics of the fluorescence decrease of Trp-65 associated with the formation of the disulfide bond were measured for T26A, H100A, H100N, D107A, R116L, and N119A MsrBs at 25 °C in buffer A on an SX18MV-R stopped-flow apparatus (Applied PhotoPhysics) adjusted for fluorescence measurements, as described previously (26). The excitation wavelength was set at 291 nm, and the emitted light was collected above 320 nm, using a cutoff filter. One syringe contained mutated MsrB in buffer A (10  $\mu\text{M}$  final concentration after mixing), and the other one contained AcMetSONHMe at various concentrations in buffer A (10–600 mM, final concentration). An average of six runs was recorded at each substrate concentration. Rate constants,  $k_{\text{obs}}$ , were obtained by fitting fluorescence traces with the monoexponential equation (Equation 3), in which  $c$  represents the end point, and  $a$  represents the amplitude of the fluorescence decrease.

$$y = ae^{-k_{\text{obs}}t} + c \quad (\text{Eq. 3})$$

When saturation is obtained as it is in wild-type, T26A, H100A, H100N, D107A, and R116L MsrBs, data were fit to Equation 4 using least squares analysis to determine  $k_{\text{obs max}}$  and  $K_S$  for AcMetSONHMe, where  $S$  represents the AcMetSONHMe concentration, and  $K_S$  represents the apparent affinity constant for the substrate.

$$k_{\text{obs}} = \frac{k_{\text{obs(max)}} \times S}{K_S + S} \quad (\text{Eq. 4})$$

For H103N and H103A MsrBs, kinetics of the slow fluorescence decrease were measured at 25 °C in buffer A on an flx spectrofluorometer (SAFAS). The excitation wavelength was set at 291 nm, and the emitted light followed at 340 nm. The assay mixture contained 10  $\mu\text{M}$  of enzyme in buffer A with various concentrations of AcMetSONHMe (10–300 mM). Data were then treated using the same procedure as described above to obtain  $k_{\text{obs max}}$  and  $K_S$  values.

To determine the pseudo-second-order constant ( $k_2$ ) values, subsaturating concentrations of AcMetSONHMe were used, from 0.1 to 2 mM for wild-type, T26A, H100A, H100N, D107A, R116L, and N119A MsrBs and from 0.1 to 1 mM for H103A and

H103N MsrBs. Kinetics of the rapid fluorescence decrease were measured at 25 °C in buffer A with a stopped-flow apparatus for wild-type, D107A, and R116L MsrBs. The kinetics of the slow fluorescence decrease were measured on an flx spectrofluorometer (SAFAS) at 25 °C in buffer A for T26A, H100A, H100N, H103A, H103N, and N119A MsrBs. The slope ( $k_2$ ) of the rate constants ( $k_{\text{obs}}$ ) plotted against substrate concentration was obtained by linear fitting.

**pH Dependence of the Reductase Step Rate Constant for Wild-type and H103N MsrBs**—Kinetics of the first step were recorded by single turnover fluorescence experiments in the absence of reductant as described above. Determination of  $k_{\text{obs max}}$  and  $K_S$  values for AcMetSONHMe as a function of pH was carried out using the same procedure as described above, but replacing buffer A with polybuffer B.  $k_{\text{obs max}}$  values were plotted against pH and fit for the wild type to Equation 5, derived from a two- $pK_a$  model for a bell-shaped curve, and for H103N MsrB to Equation 6, derived from a single  $pK_a$  model for a monosigmoidal increasing curve.

In Equation 5,  $pK_{a1}$  and  $pK_{a2}$  represent the  $pK_{\text{app}}$  values governing the acid and the basic limb, respectively, and  $k'$  and  $k''$  represent the pH-independent rate constants of the mono-deprotonated and double deprotonated forms of enzyme, respectively.

$$k_{\text{max}} = \frac{k' \times 10^{-\text{pH} - pK_{a1}} + k'' \times 10^{-pK_{a1} - \text{pH}}}{10^{-pK_{a1} - pK_{a2}} + 10^{-\text{pH} - pK_{a1}} + 10^{-2\text{pH}}} \quad (\text{Eq. 5})$$

In Equation 6,  $pK_a$  represents the  $pK_{\text{app}}$ , and  $k'$  represents the maximum pH-independent rate constant of the deprotonated form of enzyme.

$$k_{\text{max}} = \frac{k'}{1 + 10^{pK_a - \text{pH}}} \quad (\text{Eq. 6})$$

**Determination of the Rate of Ac-L-Met-NHMe (AcMetNHMe) Formation by Single Turnover Quenched-flow Experiments at pH 8 for W65A and W65F MsrBs**—In the case of W65F MsrB, quenched-flow measurements were carried out at 25 °C on a SX18MV-R stopped-flow apparatus (Applied PhotoPhysics) fitted for the double-mixing mode and adapted to recover the quenched samples as described previously (20, 26). Equal volumes (60  $\mu\text{l}$ ) of a solution containing 200  $\mu\text{M}$  W65F MsrB were mixed with various concentrations of AcMetSONHMe in buffer A (from 50 to 400 mM, final concentration) and introduced in the aging loop. The mixtures were allowed to react for 40–5000 ms and quenched with 2% trifluoroacetic acid, and samples were collected in a 200- $\mu\text{l}$  loop. At each aging time, four data runs were collected, and the corresponding quenched samples were pooled in a volume of 700  $\mu\text{l}$ . Trifluoroacetic acid (100%, 50  $\mu\text{l}$ ) was subsequently added to 200  $\mu\text{l}$  of the quenched samples to obtain precipitated protein, and in parallel, quenched samples not treated with 100% trifluoroacetic acid were used to determine the protein concentration from absorbance readings at 280 nm. In the case of W65A MsrB, quenching was carried out by manual addition of trifluoroacetic acid (100%, 50  $\mu\text{l}$ ) in 200  $\mu\text{l}$  of mixture containing 200  $\mu\text{M}$  of enzyme and 200–800 mM of AcMetSONHMe in buffer A at different time intervals (30–3600 s).

## Catalytic Mechanism of MsrB Reductase Step

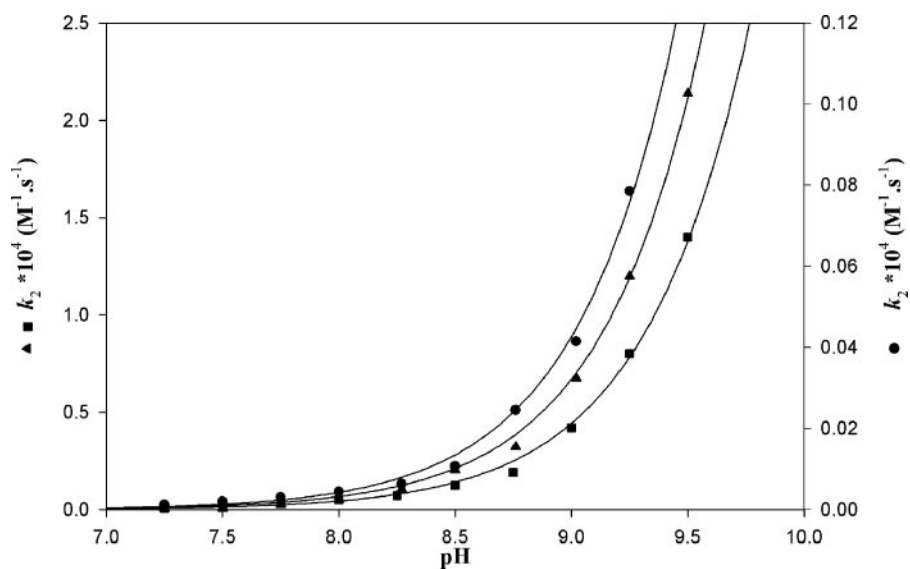


**FIGURE 2. pH dependence of the second-order rate constant  $k_2$  for the reaction of the thiol groups of wild-type, C63S, and C117S MsrBs with 2-PDS.** Kinetic reactions were performed at 25 °C under pseudo-first-order conditions at a constant ionic strength of 0.15 M over the pH range 7.25–9.5 (polybuffer B). Reactions were monitored at 343 nm in the presence of 10  $\mu\text{M}$  of wild-type MsrB and 300  $\mu\text{M}$  of 2-PDS (see also “Experimental Procedures”). Values of  $k_{\text{obs}}$  were determined at each pH using nonlinear regression analyses, and corresponding second-order rate constants  $k_2$  were plotted against pH values. The fact that saturation was not reached at  $\text{pH} \geq 9.3$  does not permit us to determine the  $\text{p}K_{\text{app}}$  and  $k_{2(\text{max})}$  values, and therefore only minimal  $\text{p}K_{\text{app}}$  and  $k_{2(\text{max})}$  values of 9.3 and  $1.5 \times 10^4 \text{ M}^{-1}\cdot\text{s}^{-1}$ , 9.3 and  $2.1 \times 10^4 \text{ M}^{-1}\cdot\text{s}^{-1}$ , and 9.0 and  $8 \times 10^2 \text{ M}^{-1}\cdot\text{s}^{-1}$  were considered for wild-type (■), C63S (▲), and C117S (●) MsrBs, respectively.

Samples treated with acetic acid were centrifuged at  $12,000 \times g$  for 30 min at room temperature. AcMetNHMe quantification in the resulting supernatant was carried out by C18 reverse phase chromatography as described previously (20, 26). Data were plotted as moles of AcMetNHMe formed per mol of MsrBs as a function of time ( $t$ ). The rate of AcMetNHMe formation was determined by fitting the curve to the monoexponential Equation 7 in which  $a$  represents the fraction of AcMetNHMe formed per mol of MsrB, and  $k_{\text{obs}}$  is the rate constant.

$$y = a(1 - e^{-k_{\text{obs}}t}) \quad (\text{Eq. 7})$$

For W65F MsrB,  $k_{\text{obs}}$  versus AcMeSONHMe concentration profile was fit to Equation 4 using least squares analysis to determine  $k_{\text{obs max}}$  and  $K_S$  for AcMetSONHMe. For W65A MsrB, the pseudo-second-order rate constant ( $k_2$ ) was obtained from the slope of rate constant ( $k_{\text{obs}}$ ) plotted against substrate concentration by linear fitting.

## RESULTS

**Rationale for the Kinetic Characterization of the Mutated MsrBs with AcMetSONHMe as Substrate**—The rate-limiting step of wild-type MsrB is associated with the Trx-recycling process (26). Therefore, to interpret the consequences on the kinetics of the reductase step of the mutated MsrBs, it was necessary to attain the rate of this step. This was done by following the decrease of the Trp-65 fluorescence emission signal intensity upon going from the reduced form to the disulfide oxidized form as described recently for the wild type (26). In this context, we assumed that the reductase step for all mutated MsrBs remain rate-determining in the process leading to the formation of the MsrB disulfide bond as demonstrated for the wild

type (26). This was verified for H100A, H100N, H103A, and H103N MsrBs by measuring directly the rate of formation of AcMetNHMe. In all cases, the rate of formation of AcMetNHMe was similar to that determined by following the decrease of the Trp-65 fluorescence intensity in the presence of 150 mM of Met-(RS)-SO (data not shown). As shown below, two types of mutated MsrBs were observed in terms of rate-limiting step as follows: those for which the rate-limiting step remains associated with the Trx-recycling process and those whose rate-limiting step precedes the Trx-recycling process. To demonstrate this, the rate of decrease in NADPH followed at 340 nm was determined under saturating concentration of Trx-TrxR-NADPH in a coupled enzymatic system and compared with that of the decrease of the Trp-65 fluorescence intensity under the same conditions of pH

(*i.e.* 8) and concentration of AcMetSONHMe.

For all mutated MsrBs,  $k_2$  values of the reductase step that represent the  $k_{\text{obs max}}/K_S$  values were determined under saturating concentrations of AcMetSONHMe. When saturating kinetics of AcMetSONHMe was observed,  $K_S$  and  $k_{\text{obs max}}$  values were determined, and  $k_2$  values were also calculated directly from these values.

In the case of mutated MsrBs at position 65, in the absence of the fluorescent Trp-65 probe, the rate of the reductase step was determined by following the rate of formation of AcMetNHMe under single turnover conditions, *i.e.* in the absence of reductant. This was done at several concentrations of AcMetSONHMe for W65A and W65F MsrBs (see Fig. 4C). In all cases, formation of  $\sim 0.8$ – $0.9$  mol of AcMetNHMe per mol of mutated MsrB was observed for all the substrate concentrations used.

The kinetic experiments were performed with AcMetSONHMe because of the better affinity of MsrB for this substrate compared with MetSO (26). Thus, the effect of the various substitutions made could be more easily quantified in terms of  $K_S$  and  $k_{\text{obs max}}$  values and not only in terms of  $k_2$  values. This proved particularly important in obtaining the pH dependence of  $k_{\text{obs max}}$  of the reductase step for wild-type, R116L, and H103N MsrBs. Indeed, to interpret the pH profile in terms of contribution of ionizable groups within the Michaelis complex, the concentration of AcMetSONHMe has to be saturating over the pH range investigated.

**Determination of the  $\text{p}K_{\text{app}}$  Value of the Catalytic Cys-117 in the Reduced Form of MsrB**—The method consisted of determining the second-order rate constant of the reaction with the Cys-specific reactivity probe 2-PDS as a function of pH, by following the formation of pyridine-2-thione at the  $\lambda_{\text{max}}$  of 343

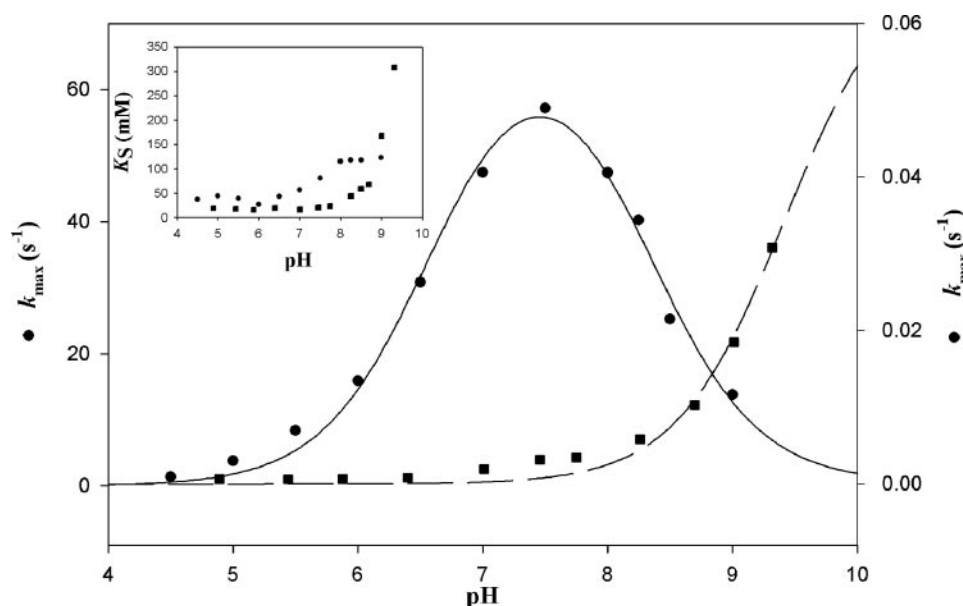


FIGURE 3. pH dependence of the reductase step rate constant  $k_{\text{obs max}}$  and of AcMetSONHMe affinity constant  $K_S$  (inset) of wild-type (●) and H103N (■) MsrBs. Kinetics of the MsrB fluorescence emission variation were followed on a stopped-flow apparatus by rapid mixing of 10  $\mu\text{M}$  enzyme final concentration and various concentrations of AcMetSONHMe at a constant ionic strength of 0.15 M over the pH range 4.5–9.3 (polybuffer B). For each pH value, experimental  $k_{\text{obs}}$  data obtained at each substrate concentration were analyzed by nonlinear regression against Equation 4 to obtain  $k_{\text{obs max}}$  and  $K_S$  values. For wild-type MsrB (●),  $k_{\text{obs max}}$  values were fit to Equation 5 (solid line) leading to a  $k'$  value of  $71 \pm 5 \text{ s}^{-1}$ , a  $k''$  value of  $0 \pm 5 \text{ s}^{-1}$ , a  $\text{p}K_{\text{a}1}$  value of  $6.6 \pm 0.1$  for the ascending limb, and a  $\text{p}K_{\text{a}2}$  value of  $8.3 \pm 0.1$  for the descending limb. For H103N MsrB (■), the fact that the plateau of the sigmoidal plot was not reached at pH 9.3 does not permit determination at the exact  $\text{p}K_{\text{app}}$  and  $k'$  values, and therefore only minimal  $\text{p}K_{\text{app}}$  and  $k'$  values of 9.0 and  $0.031 \text{ s}^{-1}$ , respectively, were considered.

**TABLE 1**  
Reductase step kinetic parameters of the wild-type and mutated MsrBs

Kinetics of the reductase step were determined in buffer A at pH 8.0 under single turnover conditions by fluorescence approach for wild-type, T26A, H100A, H100N, H103A, H103N, D107A, R116L, and N119A MsrBs and by quenched-flow experiments for W65A and W65F MsrBs as described under "Experimental Procedures." The final concentration of wild-type and mutated MsrBs was 10  $\mu\text{M}$  for fluorescence experiments and 200  $\mu\text{M}$  for quenched-flow experiments, and the AcMetSONHMe concentration varied in accord with saturation requirements (see Fig. 4). Data for wild-type, T26A, H100A, H103A, H103N, D107A, and R116L MsrBs were fit to Equation 4 by least squares regression to provide  $k_{\text{obs(max)}}$  and  $K_S$  values (see Fig. 4). For the wild-type and mutated MsrBs, pseudo-second-order rate constant  $k_2$  values were determined from the slope of the rate constant ( $k_{\text{obs}}$ ) plotted against a subsaturating substrate concentration by linear fitting (see Fig. 5). It is important to note that the  $K_S$  values have to be divided by 2 and the  $k_2$  values multiplied by 2, taking into account the fact that the *S* isomer of the sulfoxide function is neither a substrate nor an inhibitor of MsrB (17). ND indicates not determined.

	$K_S$	$k_{\text{obs max}}$	$k_{\text{obs max}}/K_S$	$k_2$
	mM	$\text{s}^{-1}$	$\text{M}^{-1}\text{s}^{-1}$	$\text{M}^{-1}\text{s}^{-1}$
Wild type	$105 \pm 5$	$49 \pm 1$	467	$474 \pm 15$
H103A	$7 \pm 1$	$(25 \pm 1) \times 10^{-4}$	0.36	$0.25 \pm 0.02$
H103N	$22 \pm 1$	$(50 \pm 5) \times 10^{-4}$	0.23	$0.9 \pm 0.1$
D107A	$64 \pm 16$	$30 \pm 3$	469	$187 \pm 5$
R116L	$22 \pm 3$	$7.0 \pm 0.2$	318	$180 \pm 5$
H100A	$180 \pm 20$	$0.7 \pm 0.1$	3.9	$1.8 \pm 0.2$
H100N	$200 \pm 40$	$0.23 \pm 0.02$	1.2	$0.9 \pm 0.1$
T26A	$240 \pm 20$	$0.7 \pm 0.1$	2.9	$2.5 \pm 0.1$
N119A	ND	ND	ND	$0.8 \pm 0.1$
W65A	ND	ND	ND	$(6.0 \pm 0.5) \times 10^{-3}$
W65F	$290 \pm 120$	$6 \pm 1$	21	ND

nm. Under native conditions, the reaction obeyed pseudo-first-order kinetics with formation of 2 mol of pyridine-2-thione per mol of MsrB. This result is in accord with the presence of the catalytic Cys-117 and the recycling Cys-63 in *N. meningitidis* MsrB. Under all conditions of pH, stopped-flow traces fitted to monoexponential Equation 1, with amplitude corresponding to

the release of 2 mol of pyridine-2-thione. The pH- $k_2$  profile fitted to monosigmoidal Equation 2 resulting in a  $\text{p}K_{\text{app}}$  value higher than 9.3 and a  $k_{2(\text{max})}$  value higher than  $1.5 \times 10^4 \text{ M}^{-1}\text{s}^{-1}$  (Fig. 2). The fact that no release of pyridine-2-thione was observed when 10 mM dithiothreitol was added showed formation of the disulfide-oxidized MsrB and not the thiopyridine adduct on each Cys (data not shown). Therefore, the  $\text{p}K_{\text{app}}$  value may be assigned to either the catalytic Cys-117, the recycling Cys-63, or to both Cys-63/Cys-117. This is dependent on the Cys that is first titrated by 2-PDS and the rate-limiting step in formation of the disulfide bond. Thus, to attain the  $\text{p}K_{\text{app}}$  of Cys-117, reactions of 2-PDS with C117S and C63S MsrBs were also carried out. Both mutated MsrBs behaved similarly to the wild-type MsrB, except that only 1 mol of pyridine-2-thione/mol of enzyme was released (curves not shown). Both pH- $k_2$  profiles were of monosigmoidal

type with no saturation at high pH, resulting in the estimation of a  $\text{p}K_{\text{app}}$  and  $k_{2(\text{max})}$  values higher than 9.3 and  $2.1 \times 10^4 \text{ M}^{-1}\text{s}^{-1}$  and 9.0 and  $0.8 \times 10^3 \text{ M}^{-1}\text{s}^{-1}$  for C63S and C117S MsrBs, respectively (Fig. 2). Altogether, the data favor a  $\text{p}K_{\text{app}}$  value of Cys-117 close to 9.3.

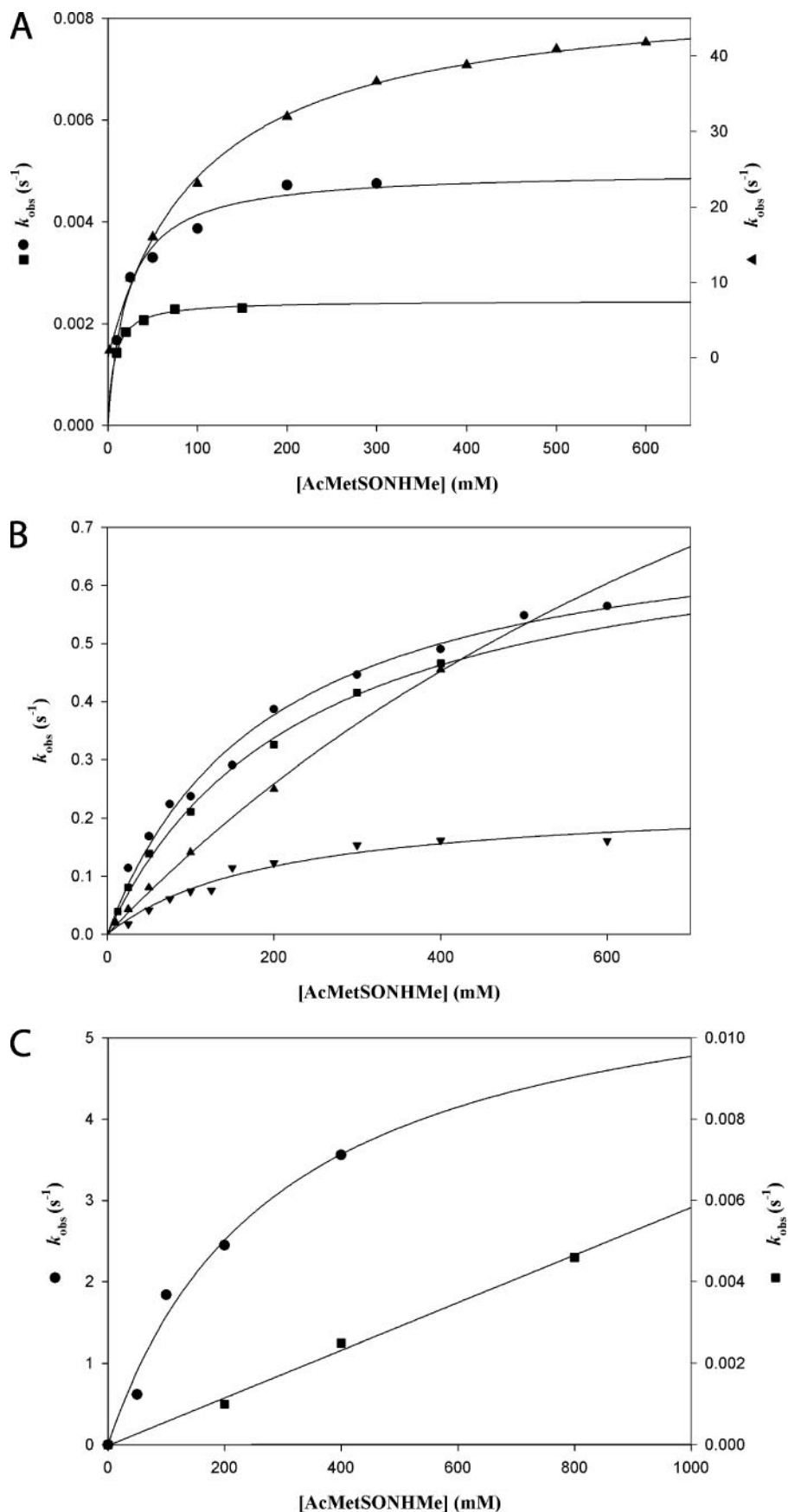
*Kinetic Investigations on the Role of Cys-117 and His-103 Directly Involved in Catalysis of the Reductase Step*—The kinetic parameters  $k_{\text{obs max}}$  and  $K_S$  of the reductase step for the wild type were determined at different pH values by fluorescence stopped-flow spectroscopy under single turnover conditions, *i.e.* in the absence of Trx. As shown in Fig. 3, the pH- $k_{\text{obs max}}$  plot is characterized by a bell-shaped profile that indicates that two groups are required to be in the proper state of ionization for maximum catalytic activity at pH 7.5. One of these groups characterized by a  $\text{p}K_{\text{app}}$  of 6.6 must be ionized, whereas the other with a  $\text{p}K_{\text{app}}$  of 8.3 has to be protonated. Substitution of His-103 by Asn and Ala resulted in a drastic effect on the rate of the reductase step. At pH 8, the  $k_{\text{obs max}}$  value, which is  $10^4$ -fold lower compared with that of the wild type (Table 1 and Fig. 4A), is similar to the rate determined under steady-state conditions ( $13 \times 10^{-4}$  and  $40 \times 10^{-4} \text{ s}^{-1}$  at 400 mM of substrate for H103A and H103N, respectively) indicating that the reductase step is now rate-limiting. The  $K_S$  value for AcMetSONHMe is in a similar range or slightly lower than that of the wild type (Table 1 and Fig. 4A). The pH- $k_{\text{obs max}}$  plot of H103N MsrB is of monosigmoidal type and showed a drastic shift in the pH profile toward the basic pH (Fig. 3). The  $\text{p}K_{\text{app}}$  value of the ascending limb is at least 9.0. Such results support the interpretation that the  $\text{p}K_{\text{app}}$  values of 6.6 and 8.3 observed for the wild type correspond to those of Cys-117 and His-103,

## Catalytic Mechanism of MsrB Reductase Step

respectively. This also indicates the following: 1) formation of the MsrB-MetSO Michaelis complex leads to an activation of Cys-117 characterized by a decreased  $pK_{app}$  of  $\sim 2.7$  pH units, whereas that of His-103 is increased by at least  $\sim 1.6$  pH units if one considers a  $pK_{app}$  of 6.7 for His-103 in the MsrB reduced form; and 2) His-103 plays an acid/base catalyst role. This is illustrated by the drastic  $k_{obs\ max}$  decrease observed not only when His-103 is substituted by Ala but also by Asn, which is an isostere of His. As mentioned in the Introduction, Lowther *et al.* (23) proposed, from the inspection of the active site in which a cacodylate molecule is bound, an activation of Cys-117 through the catalytic triad Cys-117, Arg-116, and Asp-107. In fact, when Arg-116 was substituted by Leu, the pH- $k_{obs\ max}$  profile was similar to that of the wild type (curve not shown). Only a decrease in the  $k_{obs\ max}$  value was observed over the pH range investigated. At pH 8, the  $k_{obs\ max}$  value was decreased by a factor of 7-fold (Table 1). For D107A MsrB, the  $k_{obs\ max}$  and  $K_S$  values determined solely at pH 8 are similar to those determined for the wild type (Table 1). Altogether, these results exclude any role of Arg-116 and Asp-107 in the activation of Cys-117.

*Kinetic Investigations on the Role of Thr-26, His-100, and Asn-119 in Catalysis of the Reductase Step*—Substituting Ala or Asn for His-100 led to a reductase step that becomes rate-limiting. Indeed, at pH 8, the  $k_{obs}$  values of the reductase step of H100A and H100N MsrBs determined at 400 mM of substrate, *i.e.* 0.49 and 0.21  $s^{-1}$  (Fig. 4B), are similar to those determined under steady-state conditions at 400 mM of substrate *i.e.* 0.24  $s^{-1}$  and 0.10  $s^{-1}$ , respectively. The  $k_2$  values were  $\sim 260$ - and 530-fold decreased for H100A and H100N MsrBs, respectively, compared with that of the wild type (Table 1 and Fig. 5B). These observed decreases in  $k_2$  reflect essentially a  $k_{obs}$  effect.

A pH- $k_{obs\ max}$  plot of the H100N MsrB was then done. But at a pH



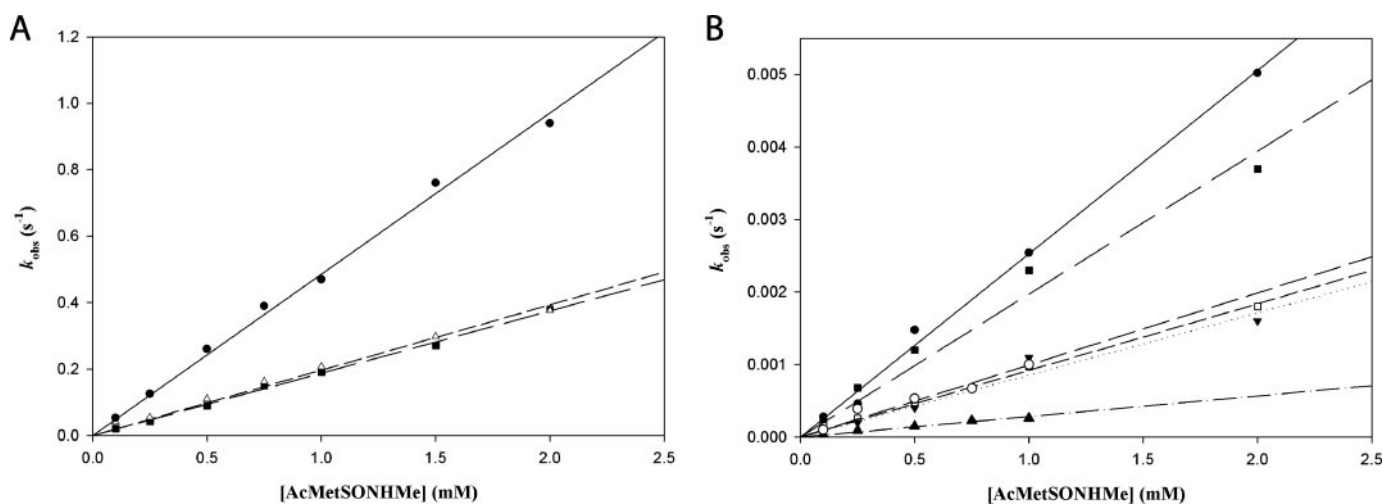


FIGURE 5. Determination of the pseudo-second-order rate constant  $k_2$  of the reductase step for wild-type, R116L, D107A (A), T26A, H100A, H100N, H103A, H103N, and N119A (B) MsrBs. The MsrB fluorescence variation was recorded on a stopped-flow apparatus for wild-type, R116L, and D107A MsrBs (A), and on a fluorimeter for T26A, H100A, H100N, H103A, H103N, and N119A MsrBs (B) as described under "Experimental Procedures." Substrate concentration ranged from 0.1 to 1 mM, and at each substrate concentration experimental data were analyzed by nonlinear regression against Equation 3 to obtain  $k_{\text{obs}}$ . The  $k_2$  values were obtained by linear fitting of  $k_{\text{obs}}$  values for wild-type (●, solid line, A), R116L (Δ, short dashed line, A), D107A (■, long dashed line, A), T26A (●, solid line, B), H100A (■, long dashed line, B), H100N (□, short dashed line, B), H103A (▲, dashed-dot line, B), H103N (○, dot-dot-dashed line, B), and N119A (▼, dotted line, B) MsrBs. All the  $k_2$  values are summarized in Table 1.

higher than 8, the  $K_S$  value for the substrate increased above 400 mM (data not shown). This prevented us from attaining a  $k_{\text{obs max}}$  value and thus determining a pH- $k_{\text{obs max}}$  plot. As a consequence, it was not possible to quantify, if any, the effect of substituting His-100 by Asn on the  $pK_{\text{app}}$  of Cys-117 and His-103.

Substituting Thr-26 by Ala led to a 190-fold decrease in the  $k_2$  value of the reductase step compared with that of the wild type, at pH 8 (Table 1 and Fig. 5B). This decrease is essentially because of a  $k_{\text{obs}}$  effect (Table 1 and Fig. 4B). At a pH higher than 8,  $K_S$  values increased significantly and therefore, as for H100N MsrB, prevented the determination of a pH- $k_{\text{obs max}}$  profile (data not shown). The fact that at pH 8 at 400 mM of substrate, the  $k_{\text{obs}}$  value of the reductase was  $0.47 \text{ s}^{-1}$  whereas under steady-state conditions the rate was  $0.2 \text{ s}^{-1}$  did not permit us to conclusively determine the nature of the rate-limiting step.

Substituting Asn-119 by Ala led to a  $k_2$  value of the reductase step, which decreases by a factor of  $\sim 600$ , at pH 8 (Table 1 and Fig. 5B). No significant saturating effect was observed up to 100 mM of substrate (Fig. 4B). At 400 mM of substrate, the  $k_{\text{obs}}$  value was  $0.45 \text{ s}^{-1}$  that has to be compared with the  $k_{\text{obs max}}$  value of  $49 \text{ s}^{-1}$  for the wild type at pH 8. As a consequence, the  $k_2$  decrease reflects essentially a  $k_{\text{obs}}$  effect accompanied by a small  $K_S$  contribution. As for the T26A MsrB, the fact that the  $k_{\text{obs}}$  of  $0.2 \text{ s}^{-1}$  determined under steady-state conditions at pH 8 is in the range of that deter-

mined for the reductase step at 400 mM of substrate does not allow the nature of the rate-limiting step to be interpreted conclusively. Again, it was not possible to obtain a pH- $k_{\text{obs max}}$  profile because of a significant increase in the  $K_S$  value above pH 8. This significant  $K_S$  increase observed for H100N, T26A, and N119A MsrBs at a pH higher than 8 compared with that of the wild type remains to be explained.

**Kinetic Investigations on the Role of the Trp-65 in the Recognition of the Substrate**—Substituting Ala for Trp-65 led to a drastic effect on the reductase step as shown by the  $10^5$ -fold decrease in  $k_2$  value determined at pH 8 (Fig. 4C). The rate-limiting step is now associated with the reductase step as supported by the fact that the  $k_{\text{obs}}$  value determined under steady-state conditions at 400 mM of substrate, *i.e.*  $1.8 \times 10^{-3} \text{ s}^{-1}$ , is similar to the  $2.5 \times 10^{-3} \text{ s}^{-1}$  value found for the reductase step at 400 mM of substrate. The  $k_2$  decrease both reflects a strong effect on  $k_{\text{obs max}}$  and  $K_S$  values. In contrast, substitution of Trp-65 by Phe led to smaller kinetic effects. The Trx-recycling process remains rate-limiting as supported by the value of  $k_{\text{obs}}$  of  $0.5 \text{ s}^{-1}$  at 400 mM of substrate that is significantly lower than the  $3.5 \text{ s}^{-1}$   $k_{\text{obs}}$  value determined for the reductase step at the same substrate concentration. The saturating kinetic effect with respect to the substrate was observed for the reductase step with  $k_{\text{obs max}}$  and  $K_S$  values of  $6 \text{ s}^{-1}$  and 290 mM values (Table 1 and Fig. 4C). Thus, substituting Phe for Trp only leads to a 8-fold decrease in  $k_{\text{obs max}}$  and 3-fold increase in  $K_S$  value at pH 8.

FIGURE 4. Determination of the catalytic parameters of the reductase step of wild-type, H103A, H103N (A), H100A, H100N, T26A, N119A (B), W65A and W65F MsrBs (C). Kinetics of the reductase step were determined in buffer A at pH 8.0 under single turnover conditions by fluorescence approach for T26A, H100A, H100N, H103A, H103N, and N119A MsrBs, and by quenched-flow experiments for W65A and W65F MsrBs as described under "Experimental Procedures." The final concentration of wild-type and mutated MsrBs was  $10 \mu\text{M}$  for fluorescence experiments and  $150 \mu\text{M}$  for quenched-flow experiments and the AcMetSONHMe concentration varied in function of the mutated MsrB tested. Experimental  $k_{\text{obs}}$  data were fit for wild-type (▲, A), H103A (■, A), H103N (●, A), H100A (●, B), H100N (▼, B), T26A (■, B), N119A (▲, B), and W65F (●, C) MsrBs to Equation 4, which gave  $k_{\text{obs max}}$  and  $K_S$  values, and for W65A (■, C) MsrB to a linear equation which gave  $k_2$  value. The catalytic parameters of wild-type and mutated MsrBs are summarized in Table 1, except for N119A MsrB. Indeed for this latter mutated MsrB, the  $k_{\text{obs max}}$  and  $K_S$  values obtained ( $1.8 \pm 0.3 \text{ s}^{-1}$  and  $1200 \pm 250 \text{ mM}$ , respectively) could only be taken as estimated due to the fact that substrate saturating concentration was not reached at 400 mM of substrate.

## DISCUSSION

As indicated in the Introduction, MsrB from *N. gonorrhoeae* in complex with a cacodylate molecule is a good model of a Met-(R)-SO-bound Michaelis complex. As shown in Fig. 1, modeling of the active site with Met-(R)-SO bound shows that methyl A of cacodylate, which is located at the bottom of the hydrophobic pocket formed by the side chains of Cys-117 and Trp-65, mimics the  $\epsilon$ -methyl, whereas the methyl B that is more toward the surface of the pocket corresponds to the  $\gamma$ -methylene group of the side chain of MetSO. The  $\epsilon$ -methyl and the  $\gamma$ -methylene groups are at a distance of  $\sim 4$  Å from the indole ring of Trp-65, and the orientation relative to the indole ring is compatible with van der Waals interactions. Modeling of the active site in which Trp-65 is substituted *in silico* by Phe suggests that the  $\epsilon$ -methyl of MetSO remains in interaction with the phenyl ring, whereas the  $\gamma$ -methylene group is too distant from the phenyl ring to provide substantial van der Waals interactions (Fig. 1). In contrast, changing Trp-65 into Ala increases the volume of the active site pocket. The absence of a hydrophobic pocket as a result of this substitution excludes any possibility of stabilization of the side chain of Met-(R)-SO, *i.e.* via its  $\epsilon$ -methyl and its  $\gamma$ -methylene groups. Therefore, no MsrB-MetSO complex productive for catalysis is predicted to be formed. That is illustrated by the drastic  $-10^5$ -fold decrease in  $k_2$  observed for W65A MsrB, which includes drastic effects both on  $K_S$  and  $k_{\text{obs max}}$ . In contrast, more productive binary complexes can be formed with W65F MsrB because of the presence of a phenyl ring that could interact with at least the  $\epsilon$ -methyl group. This is attested by the  $k_2$  value that showed only a 22-fold decrease that includes both  $K_S$  and  $k_{\text{obs max}}$  contributions. Altogether, the results show that Trp-65 is essential for the catalytic efficiency of the reductase step by optimizing the position of MetSO within the active site relative to that of the catalytic amino acids.

As proposed for the catalytic mechanism of the reductase step for MsrA, formation of an Msr-substrate complex implies a concomitant deprotonation of the catalytic Cys via an acid/base catalyst that in turn protonates the sulfoxide function and favors formation and rearrangement of the transition state of the sulfurane type, which leads to Met and sulfenic acid intermediate formation. As shown under "Results," the catalytic active MsrB form is the Cys-117<sup>-</sup>/His-103<sup>+</sup> species with  $\text{p}K_{\text{app}}$  of 6.6 and 8.3, respectively. A scenario for reduction of MetSO by MsrB can thus be proposed. Under reduced form, MsrB has its catalytic Cys-117 protonated with a  $\text{p}K_{\text{app}}$  of  $\sim 9.3$  and its His-103 under deprotonated form. Diffusion of the substrate into the active site leads to activation of Cys-117 and His-103 with transfer of the hydrogen of Cys-117 to the oxygen of the sulfoxide via His-103. Such a transfer is likely to be substrate-assisted and permits stabilization of the thiolate form of Cys-117 via the positive or partially positive charge borne by the sulfur of the sulfoxide function, which is in close spatial proximity to the sulfur of Cys-117. Clearly, our results exclude any activation of Cys-117 through a catalytic triad formed by Cys-117, Arg-116, and Asp-107. The protonated form of the sulfox-

ide function interacts by a hydrogen bonding network not only with His-103 via a strong hydrogen bond as suggested by the distance of 2.5 Å observed between the N- $\delta$  of His-103 and one of the oxygens of cacodylate but also with His-100, Asn-119, and Thr-26 via a water molecule (Fig. 1). The catalytic mechanism is likely to be concerted and leads to nucleophilic attack of the thiolate of Cys-117 on the polarized form of the sulfoxide function with formation of a sulfurane-type transition state that is stabilized by His-103 and indirectly by His-100, Asn-119, and Thr-26 via a water molecule. This transition state then evolves irreversibly to form the sulfenic acid intermediate and with subsequent Met release. The low affinity of MsrB for Met (data not shown) likely participates in the irreversibility of the reduction process.

However, major points remain to be addressed. In particular, one question concerns the way by which the proton from Cys-117 is transferred to His-103. Indeed, the distance between Cys-117 (for one of the two conformations) and His-103 in the MsrB-MetSO complex is  $\sim 6.9$  Å, considering that the MsrB-cacodylate complex is representative of the MsrB-MetSO complex. This distance is too large for direct proton transfer from Cys-117 to His-103 unless a shortening of the distance occurs upon entry and the diffusion of MetSO up to the active site or via eventually the intervention of a water molecule. Another question concerns the nature of the sulfurane transition state and how it evolves toward formation of sulfenic acid intermediate and Met.

From an evolution point of view, it is interesting to compare MsrB to MsrA in terms of catalysis and of substrate recognition. In fact, the reduction mechanism is similar for both classes of Msrs, although the active site geometries and the amino acids involved in the catalysis are different except for the catalytic Cys. In MsrB, His-103 plays an acid/base catalyst role that likely involves Glu-94 in MsrA. Both residues should also stabilize the polarized form of the sulfoxide function and the transition state. A significant difference concerns the  $\text{pH}-k_{\text{obs max}}$  profile, which is of monosigmoidal type for MsrA with assignment of the  $\text{p}K_{\text{app}}$  in the ascending limb to the catalytic Cys-51, whereas apparently Glu-94 is not titratable. In contrast, in MsrB the curve displays a bell-shaped profile, and Cys-117 but also His-103 are titratable. Such a difference remains to be explained. Differences also concern the nature of the other amino acids that stabilize the polarized form of the sulfoxide function and the transition state, the nature of the amino acids that form the hydrophobic pocket, and the 16-fold decrease in  $k_{\text{obs max}}$  of the reductase step<sup>6</sup> in MsrB when compared with MsrA. Finally, the structural/molecular factors that contribute to better binding of protein-bound MetSO rather than free MetSO remain to be characterized for both classes of Msr.

<sup>6</sup> The catalytic efficiency of the reductase step of MsrB is low, *i.e.*  $4.7 \times 10^2 \text{ M}^{-1}\text{s}^{-1}$  compared with that of MsrA, which is  $1.7 \times 10^4 \text{ M}^{-1}\text{s}^{-1}$  at pH 8.0. It is because of a  $k_{\text{obs max}}$  effect that likely results from differences in the nature of the amino acids involved in catalysis. In both cases, the affinity for the substrate is similar but low even with a substrate that mimics a protein MetSO-bound. This is the cause of the low catalytic efficiency of MsrB and even of MsrA. However, it is important to note that the rate-limiting step of both Msrs is associated with the Trx-recycling process. Therefore, saturation of the reductase step is not necessary to reach steady-state saturating conditions.

*Acknowledgments*—We thank C. Gauthier, J. Ugolini, and A. Kriznik for their very efficient technical help; Dr. A. Gruez, Dr. G. Monard, and D. M. Ruiz-Lopez for helpful discussions; Dr. G. Chevreux for mass spectrometry analyses, and Dr. M. T. Cung and C. Beaufigli for substrate NMR analyses.

## REFERENCES

- Moskovitz, J., Bar-Noy, S., Williams, W. M., Requena, J., Berlett, B. S., and Stadtman, E. R. (2001) *Proc. Natl. Acad. Sci. U. S. A.* **98**, 12920–12925
- Friguet, B. (2006) *FEBS Lett.* **580**, 2910–2916
- Petropoulos, I., and Friguier, B. (2006) *Free Radic. Res.* **40**, 1269–1276
- Stadtman, E. R., Van Remmen, H., Richardson, A., Wehr, N. B., and Levine, R. L. (2005) *Biochim. Biophys. Acta* **1703**, 135–140
- Levine, R. L., Mosoni, L., Berlett, B. S., and Stadtman, E. R. (1996) *Proc. Natl. Acad. Sci. U. S. A.* **93**, 15036–15040
- Levine, R. L., Berlett, B. S., Moskovitz, J., Mosoni, L., and Stadtman, E. R. (1999) *Mech. Ageing Dev.* **107**, 323–332
- Moskovitz, J., Flescher, E., Berlett, B. S., Azare, J., Poston, J. M., and Stadtman, E. R. (1998) *Proc. Natl. Acad. Sci. U. S. A.* **95**, 14071–14075
- Ruan, H., Tang, X. D., Chen, M. L., Joiner, M. L., Sun, G., Brot, N., Weissbach, H., Heinemann, S. H., Iverson, L., Wu, C. F., and Hoshi, T. (2002) *Proc. Natl. Acad. Sci. U. S. A.* **99**, 2748–2753
- Weissbach, H., Resnick, L., and Brot, N. (2005) *Biochim. Biophys. Acta* **1703**, 203–212
- Moskovitz, J. (2005) *Curr. Pharm. Des.* **11**, 1451–1457
- Skaar, E. P., Tobiasson, D. M., Quick, J., Judd, R. C., Weissbach, H., Etienne, F., Brot, N., and Seifert, H. S. (2002) *Proc. Natl. Acad. Sci. U. S. A.* **99**, 10108–10113
- Ejiri, S. I., Weissbach, H., and Brot, N. (1979) *J. Bacteriol.* **139**, 161–164
- Grimaud, R., Ezraty, B., Mitchell, J. K., Lafitte, D., Briand, C., Derrick, P. J., and Barras, F. (2001) *J. Biol. Chem.* **276**, 48915–48920
- Weissbach, H., Etienne, F., Hoshi, T., Heinemann, S. H., Lowther, W. T., Matthews, B., St John, G., Nathan, C., and Brot, N. (2002) *Arch. Biochem. Biophys.* **397**, 172–178
- Kauffmann, B., Aubry, A., and Favier, F. (2005) *Biochim. Biophys. Acta* **1703**, 249–260
- Boschi-Muller, S., Azza, S., Sanglier-Cianferani, S., Talfournier, F., Van Dorsselear, A., and Branlant, G. (2000) *J. Biol. Chem.* **275**, 35908–35913
- Olry, A., Boschi-Muller, S., Marraud, M., Sanglier-Cianferani, S., Van Dorsselear, A., and Branlant, G. (2002) *J. Biol. Chem.* **277**, 12016–12022
- Neiers, F., Kriznik, A., Boschi-Muller, S., and Branlant, G. (2004) *J. Biol. Chem.* **279**, 42462–42468
- Boschi-Muller, S., Olry, A., Antoine, M., and Branlant, G. (2005) *Biochim. Biophys. Acta* **1703**, 231–238
- Antoine, M., Boschi-Muller, S., and Branlant, G. (2003) *J. Biol. Chem.* **278**, 45352–45357
- Antoine, M., Gand, A., Boschi-Muller, S., and Branlant, G. (2006) *J. Biol. Chem.* **281**, 39062–39070
- Gand, A., Antoine, M., Boschi-Muller, S., and Branlant, G. (2007) *J. Biol. Chem.* **282**, 20484–20491
- Lowther, W. T., Weissbach, H., Etienne, F., Brot, N., and Matthews, B. W. (2002) *Nat. Struct. Biol.* **9**, 348–352
- Mulrooney, S. B. (1997) *Protein Expression Purif.* **9**, 372–378
- Mossner, E., Huber-Wunderlich, M., and Glockshuber, R. (1998) *Protein Sci.* **7**, 1233–1244
- Olry, A., Boschi-Muller, S., and Branlant, G. (2004) *Biochemistry* **43**, 11616–11622

**Characterization of the Amino Acids from *Neisseria meningitidis* Methionine Sulfoxide Reductase B Involved in the Chemical Catalysis and Substrate Specificity of the Reductase Step**

Fabrice Neiers, Sanjiv Sonkaria, Alexandre Olry, Sandrine Boschi-Muller and Guy Branlant

*J. Biol. Chem.* 2007, 282:32397-32405.

doi: 10.1074/jbc.M704730200 originally published online August 31, 2007

---

Access the most updated version of this article at doi: [10.1074/jbc.M704730200](https://doi.org/10.1074/jbc.M704730200)

Alerts:

- [When this article is cited](#)
- [When a correction for this article is posted](#)

[Click here](#) to choose from all of JBC's e-mail alerts

This article cites 26 references, 13 of which can be accessed free at <http://www.jbc.org/content/282/44/32397.full.html#ref-list-1>